Peer-reviewed version available at Membranes 2019, 9, 113; doi:10.3390/membranes9090113

Article

A facile synthesis of (PIM-polyimide)-(6FDA-durene-polyimide) copolymer as novel polymer membranes for CO_2 separation

Iqubal Hossain [1,2,3], Abu Zafar Al Munsur [1,2] and Tae-Hyun Kim [1,2,*]

[1] Organic Material Synthesis Laboratory, Department of Chemistry, Incheon National University, Incheon, 22012, Korea.
[2] Research Institute of Basic Sciences, Incheon National University, Incheon, 22012, Korea.
[3] Department of Chemistry, Ghent University, Sint-Pietersnieuwstraat 33,9000 Gent, Belgium

* Correspondance: tkim@inu.ac.kr (T.-H. Kim); Tel. +82-32-8358232.

Abstract: Random copolymers made of both (PIM-polyimide) and (6FDA-durene-PI) were prepared for the first time by a facile one-step polycondensation reaction. By combining the highly porous and contorted structure of PIM (polymers with intrinsic microporosity) and high thermomechanical properties of PI (polyimide), the membranes obtained from these random copolymers [(PIM-PI)*x*-(6FDA-durene-PI)y] showed high CO_2 permeability (> 1047 Barrer) with moderate CO_2/N_2 (> 16.5) and CO_2/CH_4 (> 18) selectivity, together with excellent thermal and mechanical properties. The membranes prepared from three different compositions of two comonomers (1:4, 1:6 and 1:10 of x:y), all showed similar morphological and physical properties, and gas separation performance, indicating ease of synthesis and practicability for large-scale production. The gas separation performance of these membranes at various pressure ranges (100–1500 torr) was also investigated.

Keywords: CO_2 separation, random copolymer, PIM-polyimide, permeability-selectivity, pressure effect.

1. Introduction

CO_2 separation using polymeric membranes has attracted much interest due to their easy process-ability, low energy consumption, low capital and maintenance cost, modulus compactness and environmental-friendliness relative to other separation techniques, including cryogenic distillation, amine scrubbing and pressure swing adsorption [1-5]. To this end, various types of polymer materials have been developed for the removal of CO_2 from low-quality natural gas, flue gas and syngas [2].

The key parameters used to address the intrinsic gas separation properties of specific membrane materials are their permeability (P) and selectivity (α). Briefly, permeability is a product of diffusivity (D) and solubility (S) coefficients (i.e. $P = D \times S$). The ideal selectivity ($\alpha_{A/B}$) is the ratio of permeability between two single gases (P_A and P_B), which can be depicted as $\alpha_{A/B} = P_A/P_B$. The desired membrane material for gas separation in industrial applications must have both high permeability and high selectivity. However, it is very difficult to realize both these properties in a single polymeric material. Indeed, dense polymeric membranes inevitably suffer from an undesired trade-off between gas permeability and selectivity as described by the 'Robeson upper-bound relationship' which was recently verified theoretically [6-8]. The Robeson upper-bound relationship is widely accepted as an empirical criterion by which to judge the integral performance of a newly developed polymeric membrane. With this, design of a polymer membrane with the ultimate aims of high permeability and selectivity has become the goal of researchers in this field.

The permeability of a polymer membrane is usually facilitated by the incorporation of flexible polymers such as poly[(1-trimethylsilyl)-1-propine] (**PTMSP**) [9] and polydimethylphenylsiloxane (**PDMS**) [10], but their poor selectivity and mechanical properties limited their utility in gas separation applications. Alternatively, high permeability polymer membranes can be realized by deploying stiff glassy polymer structures. These exhibit narrow distributions of free volume and high degrees of diffusivity-selectivity (D_A/D_B, where D_A and D_B refer to the diffusivity coefficient to gas A and B). Excellent mechanical properties are another feature of these rigid polymers with porous structures.

Meanwhile, the selectivity relies heavily on the solubility-selectivity and diffusivity-selectivity, $\alpha_{A/B} = S_A/S_B \times D_A/D_B$ (S_A and S_B are the solubility coefficient to gas A and B). Therefore, enhanced gas selectivity can be obtained *via* a combination of enhanced gas diffusivity selectivity and/or increased solubility of the particular gas in the polymer. Here, the diffusivity selectivity is related to the size-sieving capability of the polymer material, and relies on the mobility of the target molecule compared to those of other molecules, the structural factors such as the stiffness of the polymer chain and the degree of inter-segmental polymer chain packing [4]. The solubility selectivity, on the other hand, relies on the relative interactions between the polymer and the penetrant molecule and on the condensability levels of the penetrants to the polymer.

Among several polymer materials commercialized for gas separation, polyimides (PI)s have been most widely used because of their excellent physicochemical properties (e.g. thermal and mechanical, and chemical stability [4,10-16] with a moderate level of permeability. Moreover, these properties, including the degree of permeability, can easily be altered by varying their structures using appropriate monomers. For example, PI membranes obtained from 4,4'-hexafluoroisopropylidene di-phthalic anhydride (6FDA) demonstrated high CO_2/CH_4 separation performance capability due to inhibition of the intra-segmental mobility [4,17]. Nevertheless, most of the rigid polymers, including PIs, do not fulfil the industrial requirements of high CO_2/light gas selectivity nor of high CO_2 permeability.

Polymers of intrinsic microporosity (PIMs) have emerged as a novel polymeric membrane material for gas separation in the last decade [3,18-21]. Having a fused-ring and ladder-type contorted conformation, the unique structure of PIMs interrupt the packing of polymer chains in the solid-state, causing high free volume and low surface area. Accompanying these properties is excellent gas separation performance that surpasses Robeson's upper bounds [19,20].

Several efforts have been put forth to combine the high free volume of PIMs with the excellent physicochemical properties of PIs, and therefore, a series of PIM-polyimide (PIM-PI) homopolymers and copolymers have been attempted for gas separation [2,3,22-25]. Some of these PIM-PI copolymer membranes, in particular the multiblock-type copolymer of PIM-PI and a 6FDA-durene-based PI [(PIM-PI)*x*-*b*-(PI)y], proved to have excellent thermomechanical properties [2]. They also exhibit excellent gas separation performance, placing them well above the Robeson upper bound [2]. However, their multistep synthesis and critical control of the chain length of each block in the block copolymer remains challenging and limits their practical application for industry. Moreover, the morphology of a block copolymer is heavily dependent on the size of the individual block lengths. Even small changes of block length can affect the morphology dramatically and cause changes in the properties of the corresponding membranes. Therefore, development is still needed of more easily preparable and scalable polymers that combine the superb thermomechanical stabilities of PIs with the rigid and contorted structures of PIMs. This should increase the molecular sieving property, thereby enhancing the permeability to and selectivity for various gas pairs.

We report herein, a straightforward one-step preparation of random-type copolymers between PIM-PI and 6FDA-durene-based PI, designated as [(PIM-PI)x-(6FDA-durene-PI)y], with three different compositions (1:4, 1:6 and 1:10). We investigated the properties of the corresponding polymer membranes for CO_2 separation and performed copolymer synthesis on a 100 g scale to confirm ease of membrane synthesis and productivity.

2. Materials and Methods

Peer-reviewed version available at Membranes 2019, 9, 113; doi:10.3390/membranes9090113

2.1. Synthesis of [(PIM-PI)x-(6FDA-durene-PI)y] copolymers (1) with different compositions

A two-step synthesis (that is, polyamic acid preparation followed by imidization) was carried out to prepare the [(PIM-PI)x-(6FDA-durene-PI)y] random-type copolyimides (**1**) with three different compositions following the literature [4,15].

2.1.1. Synthesis of (PIM-PI)-(6FDA-durene-PI)(1:4)

General procedure for the synthesis of the *(PIM-PI)-(6FDA-durene-PI)(1:4):* A mixture of dianhydride monomer **(2)** (23.0 g, 36.59 mmol), 6FDA (**3**) (65.00 g, 146.36 mmol) and durene (**4**) (30.05 g, 182.95 mmol) in 150 mL of DMAc were stirred in a dried 1000 mL round bottom flask equipped with a condenser under nitrogen gas for 3 h at ice bath temperature, followed by room temperature for 12 h to form the poly(amic acid). Acetic acid (41.0 g) and triethylamine (40.69 g) were then added to this reaction mixture and the temperature of the reaction mixture was increased to 110 °C for 3 h to induce the complete imidization of poly(amic acid) into the corresponding polyimide. The highly viscous solution was then obtained by cooling to room temperature, and was then diluted with DMAc (50 mL) and precipitated into methanol (2.0 L) with stirring. Brownish-yellow polymer beads were separated by filtration, followed by washing with methanol and deionized water several times, and finally dried in a vacuum oven at 80 °C for 48 h to obtained the desired (PIM-PI)-(6FDA-durene-PI)(1:4) copolyimide with a high yield (92%); δ_H (400 MHz, $CDCl_3$); 8.09-8.02 (8H, br signal, Ar*H* **)**, 8.01-7.90 (16H, br signal, Ar*H*), 7.41-7.37 (2H, br s, Ar*H*), 7.32-7.27 (2H, br s, Ar*H*), 6.75-6.67 (2H, br s, Ar*H*), 6.41-6.33 (2H, br s, Ar*H*), 2.43-2.25 (4H, m, CH_2), 2.20-1.92 (60H, br signal, ArCH_3), 1.38-1.23 (12H, m, CCH_3); GPC ($CHCl_3$, RI)/Da M_w 4.7×10^4, PDI= 2.2; ATR-IR (cm^{-1}) 3078, 2964,2924 & 2864 (C-H stretching), 1784 (imide C=O asymmetric stretching), 1720 (imide C=O symmetric stretching), 1624, 1422 (C=C), 1352 (imide C-N stretching), 1256 (C-F stretching), 1209, 1192, 1108 (C-O-C), 748 (imide ring deformation) and 722 (C-N out of plane bending).

2.1.2. Synthesis of (PIM-PI)-(6FDA-durene-PI)(1:6)

Yield (93%); δ_H (400 MHz, $CDCl_3$); 8.09-8.02 (12H, br signal, Ar*H* **)**, 8.01-7.90 (24H, br signal, Ar*H*), 7.41-7.37 (2H, br s, Ar*H*), 7.32-7.27 (2H, br s, Ar*H*), 6.75-6.67 (2H, br s, Ar*H*), 6.41-6.33 (2H, br s, Ar*H*), 2.43-2.25 (4H, m, CH_2), 2.20-1.92 (84H, br signal, ArCH_3), 1.38-1.23 (12H, m, CCH_3); GPC ($CHCl_3$, RI)/Da M_w 4.7×10^4, PDI= 2.2; ATR-IR (cm^{-1}) 3078, 2964,2924 & 2864 (C-H stretching), 1784 (imide C=O asymmetric stretching), 1720 (imide C=O symmetric stretching), 1624, 1422 (C=C), 1352 (imide C-N stretching), 1256 (C-F stretching), 1209, 1192, 1108 (C-O-C), 748 (imide ring deformation) and 722 (C-N out of plane bending).

2.1.3. Synthesis of (PIM-PI)-(6FDA-durene-PI)(1:10)

Yield (93%); δ_H (400 MHz, $CDCl_3$); 8.10-8.04 (20H, br signal, Ar*H* **)**, 8.01-7.91 (40H, br signal, Ar*H*), 7.39-7.33 (2H, br s, Ar*H*), 7.32-7.27 (2H, br s, Ar*H*), 6.75-6.67 (2H, br s, Ar*H*), 6.41-6.33 (2H, br s, Ar*H*), 2.33-2.25 (4H, m, CH_2), 2.23-1.98 (132H, br signal, ArCH_3), 1.44-1.25 (12H, m, CCH_3);; GPC ($CHCl_3$, RI)/Da M_w 4.7×10^4, PDI = 2.2; ATR-IR (cm^{-1}) 3078, 2964, 2924 & 2864 (C-H stretching), 1784 (imide C=O asymmetric stretching), 1720 (imide C=O symmetric stretching), 1624, 1422 (C=C), 1352 (imide C-N stretching), 1256 (C-F stretching), 1209, 1192, 1108 (C-O-C), 748 (imide ring deformation) and 722 (C-N out of plane bending).

2.2. Membrane preparation

Each polymer membrane was prepared using a solution (~3 wt% in $CHCl_3$) casting technique into a flat-bottomed glass dish, followed by slow evaporation of the solvent under a minimum flow of N_2 or Ar at ambient temperature as follows. The corresponding copolyimides with different compositions (**1**) were dissolved in $CHCl_3$ (~3% w/v, g/mL), stirred at room temperature overnight

and then filtered. Each polymer solution was carefully poured into a glass dish covered with aluminium foil with small holes and allowed to undergo solvent evaporation in N_2 or Ar gas at r.t for three days. It was then placed in an oven and the solvent completely dried at 70 °C for 24 h. The dry membranes were obtained, cooled to room temperature, peeled away from the glass plate, dried again at 70 °C in an oven for 24 h, and finally stored at ambient temperature. The thickness of all the membranes was controlled to fall within the range 45 to 55 μm.

2.3. Characterization methods and measurement of gas separation performance of the membranes

All the characterizations with gas separation methods were carried out following the previous report [2,4], and are described in the supporting information.

3. Results

*3.1. Synthesis and characterization of the [(PIM-PI)x-(6FDA-durene-PI)y] copolymers (**1**)*

The random-type copolymers composed of both PIM-PI and 6FDA-durene-based PI (**1**) were prepared and were designated as [(PIM-PI)x-(6FDA-durene-PI)y]. Three different compositions (1:4, 1:6 and 1:10) of PIM-PI and 6FDA-durene-based PI were prepared by the polycondensation reaction between two dianhydride (**2** and **3**) and a diamine (**4**) monomer by targeting the monomer ratios as (1:4), (1:6) and (1:10). These were termed (PIM-PI)-(6FDA-durene-PI)(1:4), (PIM-PI)-(6FDA-durene-PI)(1:6) and (PIM-PI)-(6FDA-durene-PI)(1:10), respectively (**Scheme 1**).

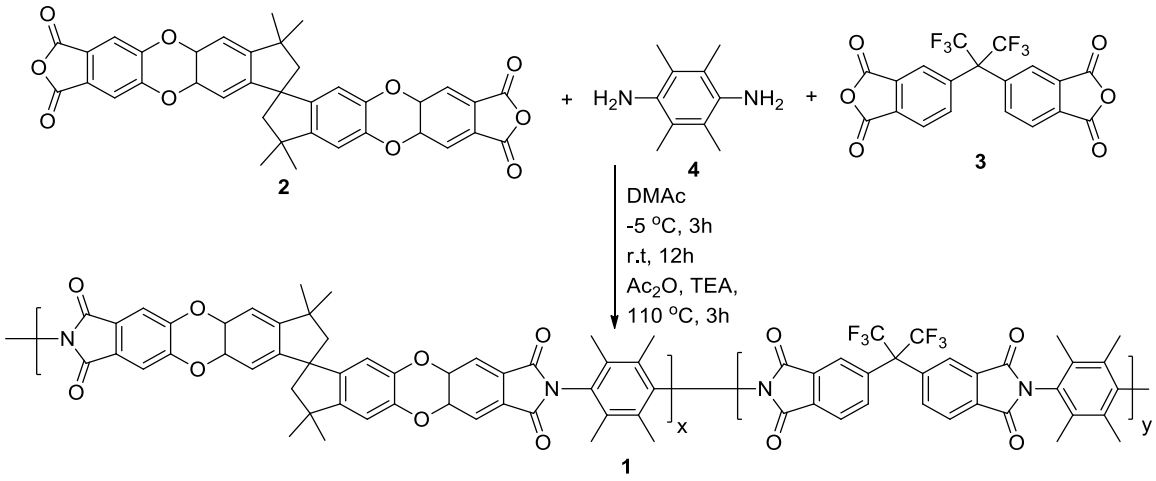

Scheme 1. Synthesis of [(PIM-PI)$_x$-(6FDA-durene-PI)$_y$] copolymers (**1**) with different x and y compositions (x:y =1:4, 1:6 and 1:10)

The structure and the composition of each copolymer, (PIM-PI)-(6FDA-durene-PI)(1:4) and (PIM-PI)-(6FDA-durene-PI)(1:6), were determined by comparing the integral ratio between two comonomers: for example, the peak integration corresponding to the phenyl proton of 6-FDA ($H_{a,b,c}$) was compared with the peak integration of the spirobisindane-based phenyl protons ($H_{1,2,3,4}$), and were found to be 1:4, 1:6 and 1:10 (**Figure 1**). In fact, the actual compositions between two comonomers were found to be the same as our feed ratio determined by theoretical calculation, indicating the validity and reliability of our random copolymer preparation. Consequently, large scale synthesis of these [(PIM-PI)$_x$-(6FDA-durene-PI)$_y$] copolymers (**1**) on 100 g scale was attempted and was successful.

Preprints (www.preprints.org) | NOT PEER-REVIEWED | Posted: 5 August 2019 doi:10.20944/preprints201908.0056.v1

Peer-reviewed version available at Membranes 2019, 9, 113; doi:10.3390/membranes9090113

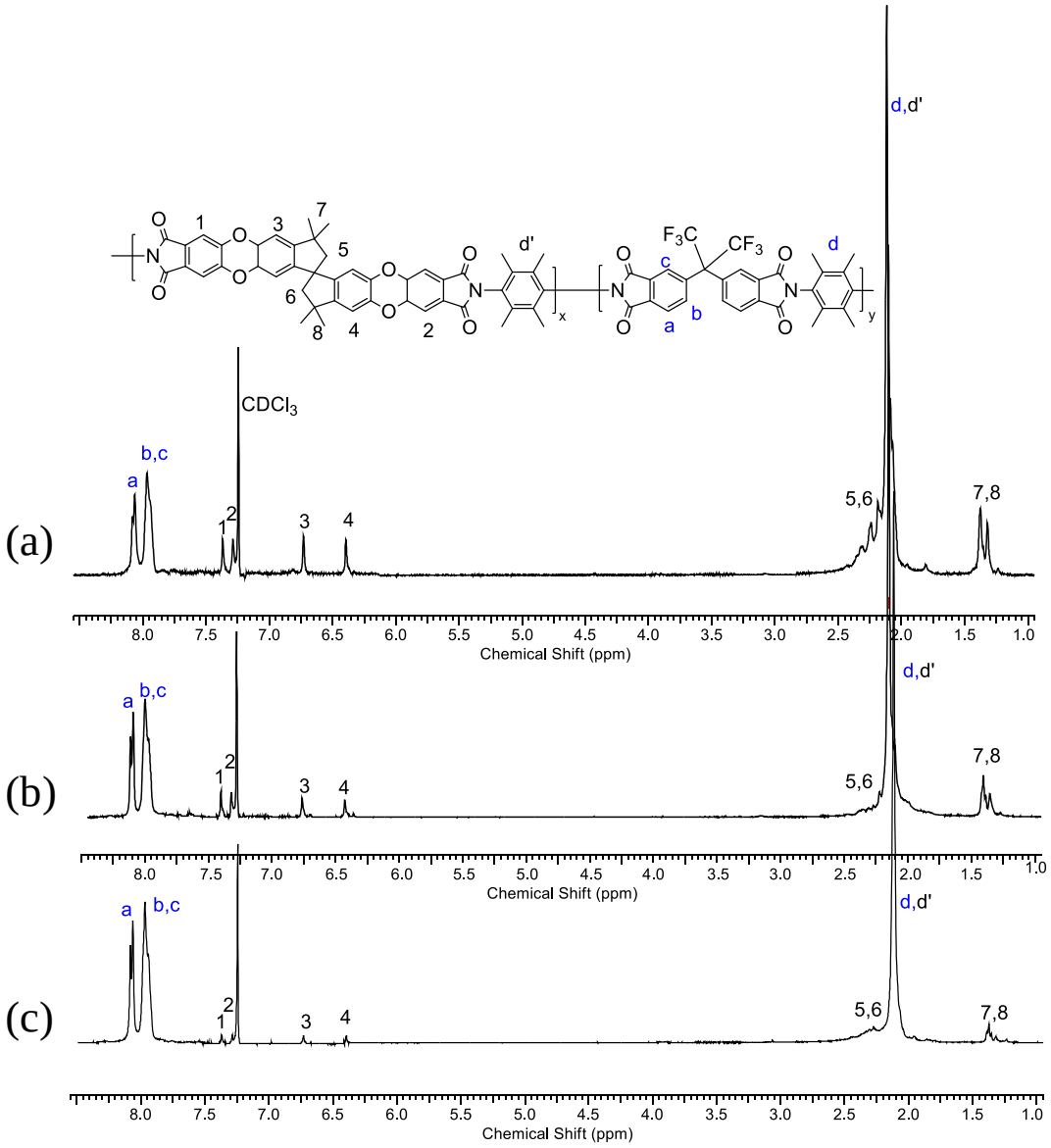

Figure 1. ^{1}H NMR spectra of the [(PIM-PI)$_x$-(6FDA-durene-PI)$_y$] copolymers with different compositions (x:y = 1:4, 1:6 and 1:10).

The structures of [(PIM-PI)$_x$-(6FDA-durene-PI)$_y$] copolymers (**1**) were further confirmed by ATR-IR spectroscopic analysis (**Figure S1,** see supporting information), by showing peaks around 1780 and 1720 cm^{-1} corresponding to both asymmetric and symmetric stretching for imide C=O absorption, and peaks at 1350 (imide C-N stretching), 1256 (C-F), 742 (imide ring deformation) and 726 (C-N out of plane bend), all indicating successful synthesis of the desired copolyimides.

The molecular weights (M_w) of the three [(PIM-PI)$_x$-(6FDA-durene-PI)$_y$] copolymers were determined by gel permeation chromatography (GPC), and were found to be in the range 43–49 kDa, supporting the achievement of copolymerization (**Table 1**).

Table 1. Various physical properties of the [(PIM-PI)$_x$-(6FDA-durene-PI)$_y$] copolymers and their corresponding membranes

Copolymer composition	Molecular weight (kDa)		ϱ (g.cm^{-3})	d-spacing (Å)
	M_w	PDI		

(x:y)(1:4)	47.0	2.20	1.29	7.04, 12.72
(x:y)(1:6)	48.8	1.74	1.30	6.98, 11.96
(x:y)(1:10)	42.7	1.26	1.32	6.92

3.2. Preparation of the [(PIM-PI)x-(6FDA-durene-PI)y] copolymer membranes

The [(PIM-PI)$_x$-(6FDA-durene-PI)$_y$] copolymer membranes with three different compositions, denoted as (PIM-PI)-(6FDA-durene-PI)(1:4), (PIM-PI)-(6FDA-durene-PI)(1:6) and (PIM-PI)-(6FDA-durene-PI)(1:10), were prepared using the solution-casting method with $CHCl_3$ solution of each polymer to give flexible membranes with thickness of ~45-55 μm (**Figure 2**). All three membranes were readily soluble in organic solvents such as $CHCl_3$, $CHCl_2$, THF, and DMF, but were sparingly soluble in DMSO.

Figure 2. Pictures of the [(PIM-PI)x-(6FDA-durene-PI)y] copolymer membranes with 1:4 (a), 1:6 (b) and 1:10 (c) compositions.

3.3. Morphological analysis by XRD and AFM

The morphologies of the three copolymer membranes were investigated using wide-angle X-ray diffraction (WAXD) and atomic force microscopy (AFM) in order to determine crystallinity and intermolecular chain distance of the polymers.

Figure 3 shows the WAXD data of the [(PIM-PI)-(6FDA-durene-PI)(1:4), (PIM-PI)-(6FDA-durene-PI)(1:6) and (PIM-PI)-(6FDA-durene-PI)(1:10)] copolymer membranes. Similar patterns of broad peaks were observed for all membranes, suggesting amorphous structures. The polymer-polymer chain distance (or d-spacing), was further estimated using Bragg's law, $d = \lambda / 2 \sin \theta$ (λ: the wavelength of 1.789 Å; θ: the scattering angle) (**Table 1**). Again, similar d-spacing values [7.03 Å for (PIM-PI)-(6FDA-durene-PI)(1:4), 6.98 Å for (PIM-PI)-(6FDA-durene-PI)(1:6) and 6.92 Å for (PIM-PI)-(6FDA-durene-PI)(1:10)] were observed. These results suggest that the gas separation properties of both membranes would be similar with only small variation. In addition, an additional peak at around 12.7 Å was observed for (PIM-PI)-(6FDA-durene-PI)(1:4) and (PIM-PI)-(6FDA-durene-PI)(1:6), which had more PIM-PI unit content. This additional peak is thought to arise from the distance between neighbouring spiro-carbon atoms in the PIM structure [2,26], but for the (PIM-PI)-(6FDA-durene-PI)(1:10) the peak was not obtained due to its very low PIM-PI content.

Peer-reviewed version available at Membranes 2019, 9, 113; doi:10.3390/membranes9090113

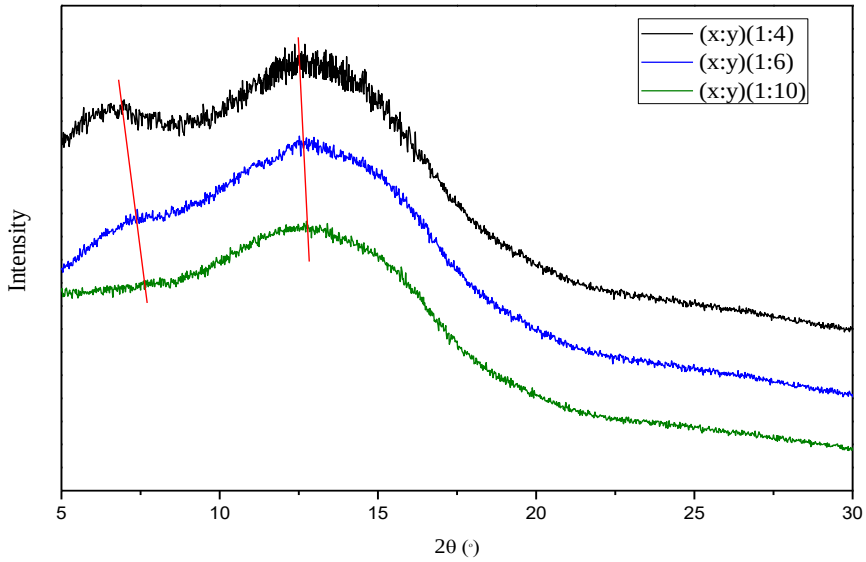

Figure 3. Wide-angle XRD diagrams of the [(PIM-PI)x-(6FDA-durene-PI)y] copolymers with different compositions

Moreover, similar morphologies without phase separation were also observed for all three copolymer membranes using AFM (**Figure 4a, 4b and 4c**), indicating that the highly porous permeable PIM-PI unit is randomly distributed over the less permeable 6FDA-durene-PI domain.

From the above morphological analyses, it was expected that the gas separation performance of the copolymer compositions (PIM-PI)-(6FDA-durene-PI)(1:4) and (PIM-PI)-(6FDA-durene-PI)(1:6) would be very similar, with slightly higher permeability for the former. In contrast, the gas permeability of (PIM-PI)-(6FDA-durene-PI)(1:10) composition was expected to be lower than the other two compositions based on the comparatively lower d-spacing in its microstructure.

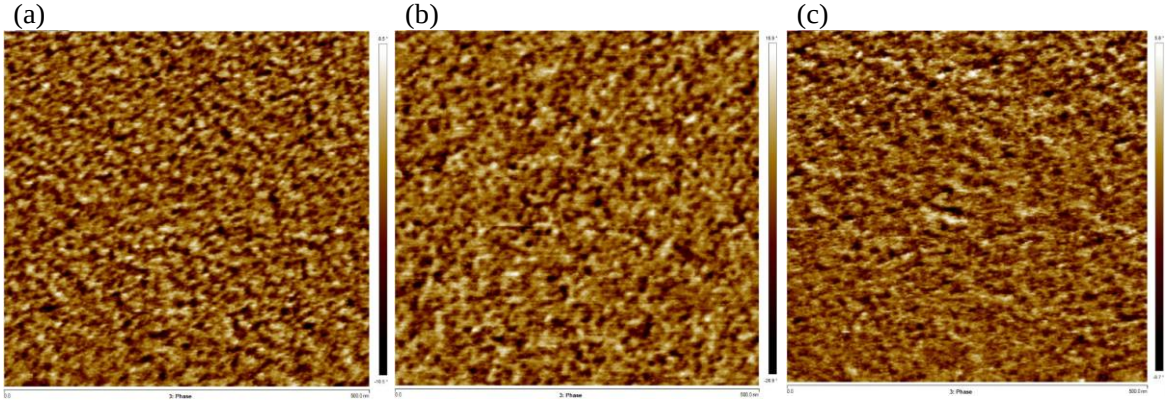

Figure 4. AFM images of the (PIM-PI)-(6FDA-durene-PI)(1:4) (a) and (PIM-PI)-(6FDA-durene-PI)(1:6) (b) and (PIM-PI)-(6FDA-durene-PI)(1:6) (c)

3.4. Gas separation performance of the copolymer membranes

The pure gas separation properties of the obtained three [(PIM-PI)x-(6FDA-durene-PI)y] (x:y = 1:4, 1:6 and 1:10) copolymer membranes were determined at 30 °C and 2 atm pressure using the constant-volume/variable-pressure method (**Table 2**).

Table 2. Gas permeability[a] and selectivity of the [(PIM-PI)x-(6FDA-durene-PI)y] copolymer membranes at 30 °C and 2 atm pressure.

Copolymer composition	Permeability			Selectivity	
	P_{CO2}	P_{N2}	P_{CH4}	$\alpha_{CO2/N2}$	$\alpha_{CO2/CH4}$
(x:y)(1:4)	1265	74.1	69.4	17.05	18.23
(x:y)(1:6)	1225	73.7	68.8	16.58	17.81
(x:y)(1:6)	1047	64.4	60.2	16.25	17.39

[a] Permeability in Barrer, where 1 Barrer = 10^{-10} [cm^3 (STP) cm][cm^{-2} s^{-1} cm^{-1} Hg^{-1}]

It is apparent that the copolymers with all three different compositions [(PIM-PI)-(6FDA-durene-PI)(1:4), (PIM-PI)-(6FDA-durene-PI)(1:6) and (PIM-PI)-(6FDA-durene-PI)(1:10)] exhibited higher CO_2 permeability (> 1047 Barrer) relative to other gases (i.e. N_2 and CH_4) as follows: CO_2 >> N_2 > CH_4. This order in permeabilities can be explained by the diffusivity, which takes the same order: CO_2 >> N_2 > CH_4, as shown in **Table 3** and **Figure 5**. Thus, the order of diffusivity is determined by the kinetic diameter of the penetrant gases, which is inversely proportional to the gas molecule size [CO_2 (3.30 Å) < N_2 (3.64 Å) < CH_4 (3.80 Å)]; that is, smaller gases diffuse through the polymer matrix faster than larger gases do.

Table 3. Gas diffusivity[a] and solubility[b] of the (PIM-PI)x-(6FDA-durene-PI)y copolymer membranes at 30 °C and 2 atm pressure

Copolymer composition	Diffusivity			Solubility		
	P_{CO2}	**P_{N2}**	**P_{CH4}**	**S_{CO2}**	**S_{N2}**	**S_{CH4}**
(x:y)(1:4)	29.4	17.0	4.9	0.431	0.046	0.143
(x:y)(1:6)	28.8	16.9	4.8	0.426	0.045	0.142
(x:y)(1:10)	25.1	14.6	4.3	0.417	0.044	0.140

[a] Diffusivity coefficient (10^{-8} cm^2/s); [b] Solubility coefficient (cm^3 (STP)/cm^3 cmHg).

It is noteworthy that the performance of our newly-developed (PIM-PI)x-(PI)y copolymer membranes is much higher than most of the PIs reported in the literature[4,510,17], due to the incorporation of the highly permeable microporous PIM unit, resulting in enhanced solubilities of the penetrants in the newly-developed copolymers. For example, the solubilities of all the gases in the present studies were much higher than those of 6FDA-durene-PI (S = 0.17, 0.02 and 0.06 for CO_2, N_2 and CH_4, respectively), which is a highly permeable PI [4].

Preprints (www.preprints.org) | NOT PEER-REVIEWED | Posted: 5 August 2019 doi:10.20944/preprints201908.0056.v1

Peer-reviewed version available at Membranes 2019, 9, 113; doi:10.3390/membranes9090113

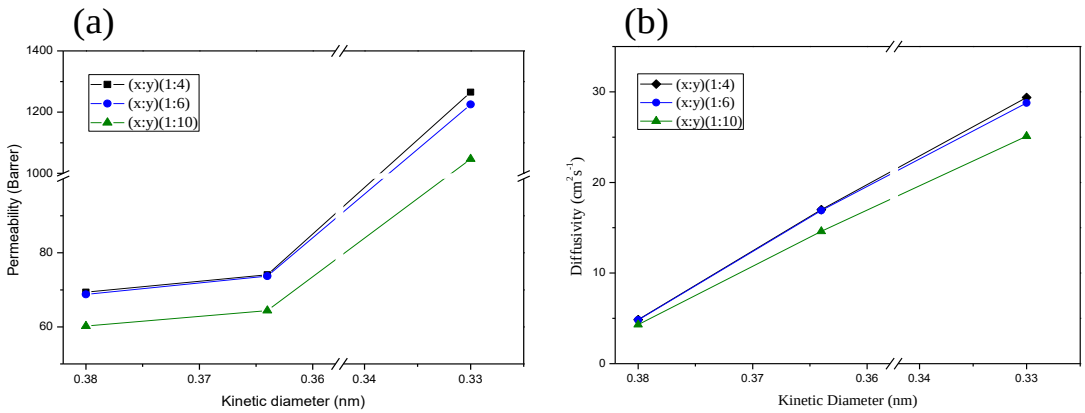

Figure 5. Gas permeability (a) and diffusivity (b) of the (PIM-PI)x-(6FDA-durene-PI)y copolymer membranes as a function of the kinetic diameter of the gas molecules

When we compare the gas separation properties of the (PIM-PI)x-(6FDA-durene-PI)y copolymer membranes according to the three different compositions (1:4, 1:6 and 1:10), we find that two polymers (1:4 and 1:6) show very similar permeability and selectivity. Slightly higher CO_2-permeability and selectivity were observed for (PIM-PI)-(6FDA-durene-PI)(1:4), which has higher PIM-PI content, than for (PIM-PI)-(6FDA-durene-PI)(1:6) (**Table 3**). It was expected that the highly microporous PIM unit would not only enhance the permeability, but would also increase the selectivity due to its enhanced solubility as well as the diffusivity of this unique structure. Nevertheless, the difference in the permeability between the two copolymers (1:4 and 1:6) was small, and this is ascribed to the random distribution of the highly permeable unit (PIM-PI) of the copolymer in the low permeable domain. This notion is supported by morphological analyses using both XRD and AFM. On the other hand, the permeability of the (PIM-PI)-(6FDA-durene-PI)(1:10) polymer showed lower permeability than the other two compositions did due to the lowest content of highly permeable PIM-PI in its structure. Nevertheless, the permeability of (PIM-PI)-(6FDA-durene-PI)(1:10) was still high (1047 Barrer) compared to other rigid PI-type polymers reported. This is certainly a great advantage of random-type copolymers because, as mentioned earlier, the changes of the morphology and the physical properties, together with gas separation performance, according to changes in the composition are significant for the typical block-type copolymers [2].

Moreover, the present random-type PIM-PI copolymers displayed moderate selectivity of CO_2/CH_4, which is a common feature of most glassy polymers (e.g. PIs, PES, PEK and PPO), in which diffusivity selectivity has more influence than solubility selectivity does (**Table 4**). On the other hand, the moderate permselectivity of CO_2/N_2 was mainly influenced by solubility selectivity (**Table 4**), which feature is similar in most of the PIM-based glassy polymer membranes. Therefore, the perceptive combination of these two different compositions mutually enhanced the selectivity of the two pairs of gases: CO_2/CH_4 and CO_2/N_2.

Table 4. Gas diffusivity selectivity and solubility selectivity of the (PIM-PI)x-(6FDA-durene-PI)y copolymer membranes at 30 °C and 2 atm pressure

Copolymer composition	Diffusivity Selectivity		Solubility Selectivity	
	$D_{CO2/CH4}$	$D_{CO2/N2}$	$S_{CO2/CH4}$	$S_{CO2/N2}$
(x:y)(1:4)	6.06	1.73	3.01	9.48
(x:y)(1:6)	5.95	1.70	3.00	9.47
(x:y)(1:10)	5.84	1.71	2.98	9.45

Preprints (www.preprints.org) | NOT PEER-REVIEWED | Posted: 5 August 2019 doi:10.20944/preprints201908.0056.v1

Peer-reviewed version available at Membranes 2019, 9, 113; doi:10.3390/membranes9090113

3.5. Permeability vs selectivity

As mentioned earlier, the trade-off relationship between permeability (P) and ideal selectivity (α) is a common phenomenon for most polymer membrane-based gas separation (i.e. higher permeability is obtained at the cost of reduced selectivity and vice versa). The CO_2 permeability versus the CO_2/CH_4 (**Figure 6a**) and CO_2/N_2 **(Figure 6b**) selectivity values of the newly developed [(PIM-PI)x-(6FDA-durene-PI)y] membranes were then placed at the upper bound of the Robeson plots, and compared with the reported values obtained from the typical PIs [4,5,10,15,17], together with PIM-PI type homo- and copolymers [3,23-25]. The comparison results showed that our random-type [(PIM-PI)x-(6FDA-durene-PI)y] copolymers outperformed most of the PIs and PIM-PI homopolymers (**Figure 6a**). Furthermore, the trade-off results of the [(PIM-PI)x-(6FDA-durene-PI)y] copolymers crossed the upper bound line of 1991 for CO_2/CH_4, although they were still below the upper bound limit of 2008.

In contrast, all random-type copolymer membranes fell below the upper bound for CO_2/N_2, but still showed better performance than PIs did (**Figure 6b**).

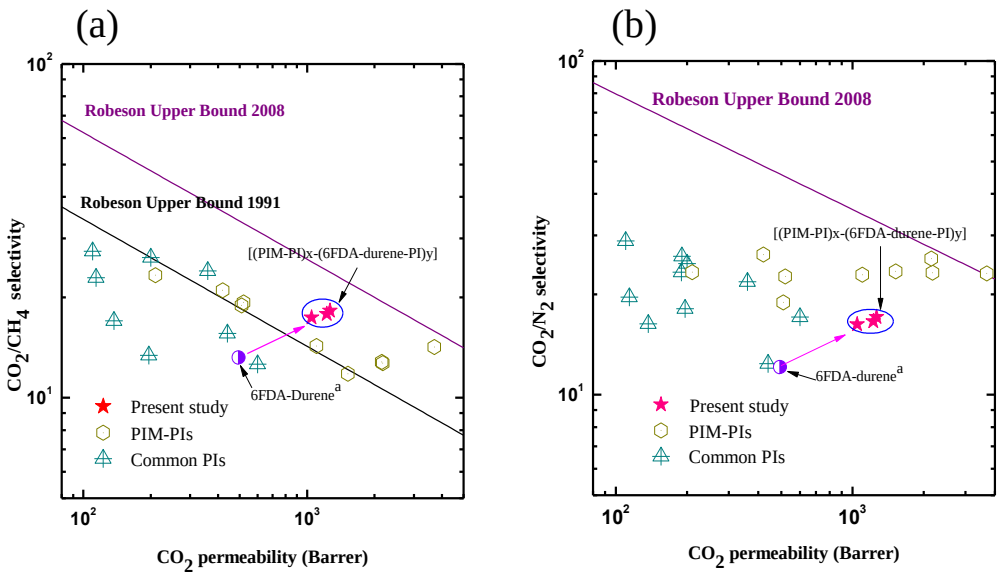

Figure 6. 'Robeson upper bound' plots comparing the CO_2/CH_4 (a) and CO_2/N_2 (b) separation performance capabilities of the block copolymer membranes with other reported PIM-PIs and common PIs; data taken from [3-7,10,13,15,17,23-25].

3.6. Pressure effect on permeability

Due to its having the best gas separation performance, the (PIM-PI)-(6FDA-durene-PI)(1:4) copolymer membrane was further investigated for the effect of feed pressure on its gas-separation ability over a feed pressure range of 100–15.00 Torr (0.1–2 bar) at 30 °C (**Figure 7**). It was observed that the CO_2 permeability increased dramatically with decrease in the pressure, while the CH_4 and N_2 permeability slightly increased with decrease in the feed pressure (**Figure 7a**). Therefore, the decrease in the CO_2/CH_4 and CO_2/N_2 selectivity that occurred at higher pressure was mainly due to decreased CO_2 permeability (**Figure 7b**). A similar result was reported elsewhere [26-30]. This trend of gradual decrease in permeability with increasing pressure was also observed for other microporous rigid polymers and is ascribed to the filling of the sorption sites in the Langmuir model at a higher pressure range[28-31]. This excellent separation performance at low pressure probably originates from stronger interaction between CO_2 and Langmuir cavities than with other gases due

Preprints (www.preprints.org) | NOT PEER-REVIEWED | Posted: 5 August 2019 doi:10.20944/preprints201908.0056.v1

Peer-reviewed version available at Membranes 2019, 9, 113; doi:10.3390/membranes9090113

to its quadrupole moment and molecular size. This results in its gradual saturation with increasing pressure; as a result, separation performance decreases at high pressure.

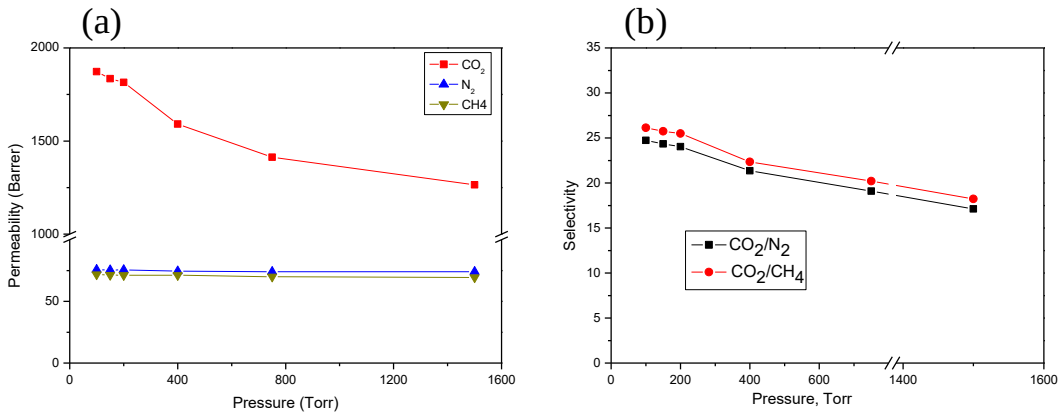

Figure 7. Gas permeability (a) and selectivity (b) of the (PIM-PI)-(6FDA-durene-PI)(1:4) membrane at various pressure ranges

All the gas separation properties strongly indicate that the newly developed [(PIM-PI)x-(6FDA-durene-PI)y] random-type copolymers are promising candidate materials to be used for CO_2 separation, particularly at, but not only limited to, low pressures.

3.7. Thermal and mechanical properties

Finally, the thermal and mechanical properties of the (PIM-PI)x-(6FDA-durene-PI)y copolymer membranes were investigated (**Table 5** and **Figure S2).**

TGA analysis showed that both copolymers had high thermal stability with initial decomposition temperatures above 465 °C, with the maximum weight loss temperature and residual weight loss, $\mathbf{T_{max}}$ and **RW**, at 536 °C and > 53%, respectively. This indicates excellent thermal stability, suitable for applications requiring high-temperature CO_2 separation, of our (PIM-PI)x-(6FDA-durene-PI)y copolymer membranes (**Figure S2a** and **Table 5**).

The mechanical stability of the copolymer membranes was further analysed by measuring the stress-strain values of the all membranes at 50% RH (**Figure S2b** and **Table 5**). All three membranes exhibited excellent tensile strength of more than 70 MPa and Young's modulus value > 2.0 GPa: higher than those of PIM-1 [32] and PIM-PI-1 homopolymer [24]**.** Incorporation of the 6FDA-durene-based PI unit onto the PIM-PI unit was, therefore, believed to enhance the mechanical stability of the corresponding [(PIM-PI)x-(6FDA-durene-PI)y] copolymer membranes, as we originally intended.

Table 5. Thermal and mechanical properties of the copolymer membranes.

Polymer code	Decomposition temperature				Tensile strength, (MPa)	Elongation at break, (%)	Young's Modulus, (GPa)
	T_d (°C)	T_5 (°C)	T_{max} (°C)	RW (%)			
(x:y)(1:4)	464	494	536	53.14	71.1	6.9	2.92
(x:y)(1:6)	470	497	538	54.32	79.0	7.1	2.80
(x:y)(1:10)	480	506	545	57.63	82.7	9.4	2.01

5. Conclusions

A series of random-type [(PIM-PI)*x*-(6FDA-durene-PI)y] copolymers with different composition (x;y = 1:4, 1:6 and 1:10) were synthesized for the first time using a facile one-step polycondensation reaction. By combining the highly porous and contorted structure of PIM with the excellent thermomechanical properties of polyimide, the membranes obtained from these random-type [(PIM-PI)*x*-(6FDA-durene-PI)y] copolymers showed very high CO_2 permeability (> 1047 Barrer) with moderate CO_2/N_2 (over 16.3) and CO_2/CH_4 (over 18) selectivity, together with excellent thermal and mechanical properties. The membranes prepared from three different compositions of comonomers (1:4, 1:6 and 1:10 of x:y), showed similar morphological and physical properties, and only slightly different gas separation performance. This indicates ease of synthesis and practicality for large-scale production. Last but not least, the fruitful result of separation performance over a wide pressure range (100–1500 torr) also makes the new polymer appear a competitive material for applications requiring CO_2 separation.

Supplementary Materials: The following are available online at www.mdpi.com/xxx/s1, Figure S1: ATR-FTIR spectra of the [(PIM-PI)$_x$-(6FDA-durene-PI)$_y$] copolymers with three different compositions (x:y = 1:4, 1:6 and 1:10), Figure S2: (a) TGA graph and (b) S-S curve of the copolymer [(PIM-PI)$_x$-(6FDA-durene-PI)$_y$] membranes, Materials, Characterizations and measurements, Gas permeation procedure etc.

Author Contributions: Conceptualization, I. H. and T.-H. Kim; methodology, I. H. and A. Z. A M.; software, I. H.; validation, I. H., A. Z. A M. and T.-H. Kim; formal analysis, I. H.; investigation, I. H. and A. Z. A M.; resources, I. H. and A. Z. A M.; data curation, I. H. and T.-H. Kim; writing—original draft preparation, I. H.; writing—review and editing, T.-H. Kim; visualization, I. H.; supervision, T.-H. Kim; project administration, T.-H. Kim; funding acquisition, T.-H. Kim.

Funding: This research was funded by Basic Science Research Program through the National Research Foundation of Korea (NRF) funded by the Ministry of Education (NRF-2017R1A6A1A06015181).

Acknowledgments: The authors acknowledge Dr. S. Y. Park of the Research Institute of Basic Sciences at INU for her assistance in analysing the AFM images of the membranes

Conflicts of Interest: The authors declare no conflict of interest.

References

1. Rao, A.B.; Rubin, E.S. A Technical , Economic, and Environmental Assessment of Amine-Based CO_2 Capture Technology for Power Plant Greenhouse Gas Control. *Energy Environ. Sci.* **2002**, *412*, 4467–4475.
2. Hossain, I.; Yong, S.; Rizzuto, C.; Barbieri, G.; Tocci, E; Kim, T.-H. PIM-Polyimide Multiblock Copolymer-Based Membranes with Enhanced CO_2 Separation Performances. *J. Memb. Sci.* **2019**, *574*, 270–281.
3. Wang, S.; Li, X.; Wu, H.; Tian, Z.; Xin, Q.; He, G.; Peng, D.; Chen, S.; Yin, Y.; Jiang, Z.; Guiver, M.D. Advances in High Permeability Polymer-Based Membrane Materials for CO_2 Separations. *Energy Environ. Sci.* **2016**, *9*, 1863–1890.
4. Hossain, I.; Zafar, A.; Munsur, A.Z.A; Choi, O.; Kim, T.-H. Bisimidazolium PEG-Mediated Crosslinked 6FDA-Durene Polyimide Membranes for CO_2 Separation. *Sep. Purif. Technol.* **2019**, *224*, 180–188.
5. Du, N.; Park, B.P.; Dal-Cin, M.M.; Guiver, M.D. Advances in High Permeability Polymeric Membrane Materials for CO_2 Separation. *Energy Environ. Sci.* **2012**, 7306–7322.
6. Robeson, L.M. Correlation of Separation Factor versus Permeability for Polymeric Membranes. *J. Memb. Sci.* **1991**, *62*, 165–185.
7. Robeson, L.M. The Upper Bound Revisited. *J. Memb. Sci.* **2008**, *320*, 390–400.
8. Freeman, B.D. Basis of Permeability/Selectivity Tradeoff Relations in Polymeric Gas Separation Membranes. *Macromolecules* **1999**, *32*, 375–380.
9. Dai, Z.; Loining, V.; Deng, J.; Ansaloni, L.; Deng, L. Poly(1-trimethylsilyl-1-propyne)-Based Hybrid Membranes: Effects of Various Nanofillers and Feed Gas Humidity on CO2 Permeation. *Membranes* **2018**, 8, 1-19.

10. You, H.; Hossain, I.; Kim, T.-H. Piperazinium-mediated crosslinked polyimidepolydimethylsiloxane (PI-PDMS) copolymer membranes: the effect of PDMS content on CO_2 separation. *RSC Adv.* **2017**, *8*, 1328–1336.
11. Li, H.; Zhang, S.; Gong, C.; Liang, Y.; Qi, Z.; Li, Y. Novel High T_g, Organosoluble Poly (ether imide)s Containing 4,5-Diazafluorene Unit: Synthesis and Characterization. *Eur. Polym. J.* **2014**, *54*, 128–137.
12. Dhara, M.G.; Banerjee, S. Fluorinated High-Performance Polymers : Poly (Arylene Ether) s and Aromatic Polyimides Containing Trifluoromethyl Groups. *Prog. Polym. Sci.* **2010**, *35*, 1022–1077.
13. Cecopieri-Gomez, M.L; Palacios-Alquisira, J; Domiınguez, J.M. On the Limits of Gas Separation in CO_2/CH_4 , N_2/CH_4 and CO_2/N_2 Binary Mixtures Using Polyimide Membranes. *J. Memb. Sci.* **2007**, *293*, 53–65.
14. Gye, B.; Kammakakam, I.; You, H.; Nam, S.; Kim, T.-H. PEG-Imidazolium-Incorporated Polyimides as High-Performance CO_2-selective Polymer Membranes : The Effects of PEG-Imidazolium Content. *Sep. Purif. Technol.* **2017**, *179*, 283–290.
15. Kammakakam, I.; Yoon, H.W.; Nam, S.; Park, H.B.; Kim, T.-H. Novel Piperazinium-Mediated Crosslinked Polyimide Membranes for High Performance CO_2 Separation. *J. Memb. Sci.* **2015**, *487*, 90–98.
16. O'Harra, K.E.; Kammakakam, I.; Devriese, E.M.; Noll, D.M.; Bara, J.E.; Jackson, E. M. Synthesis and Performance of 6FDA-Based Polyimide-Ionenes and Composites with Ionic Liquids as Gas Separation Membranes. *Membranes* **2019**, *9*, 1-17.
17. Kim, T.H.; Koros, W.J.; Husk, G.R.; O'Brien, K.C. Relationship between Gas Separation Properties and Chemical Structure in a Series of Aromatic Polyimides. *J. Memb. Sci.* **1988**, *37*, 45–62.
18. Staiger, C.L.; Pas, S.J.; Hill, A.J.; Cornelius, C.J. Gas Separation, Free Volume Distribution, and Physical Aging of a Highly Microporous Spirobisindane Polymer. *Chem. Mater.* **2008**, *20*, 2606–2608.
19. Song, J.; Du, N.; Dai, Y.; Robertson, G.P.; Guiver, M.D.; Thomas, S.; Pinnau, I. Linear High Molecular Weight Ladder Polymers by Optimized Polycondensation of Tetrahydroxytetramethylspirobisindane and 1,4-Dicyanotetrafluorobenzene. *Macromolecules* **2008**, *41*,7411–7417.
20. Budd, P.M.; Msayib, K.J.; Tattershall, C.E.; Ghanem, B.S.; Reynolds, K.J.; Mckeown, N.B.; Fritsch, D. Gas Separation Membranes from Polymers of Intrinsic Microporosity. *J. Membr. Sci.* **2005**, *251*, 263–269.
21. Budd, P.M.; Elabas, E.S.; Ghanem, B.; Makhseed, S.; McKeown, N.B.; Msayib, K.J.; Tattershall, C.E.; Wang, D. Solution-Processed, Organophilic Membrane Derived from a Polymer of Intrinsic Microporosity. *Adv. Mater.* **2004**, *16*, 456–459.
22. Ghanem, B.S.; Mckeown, N.B.; Budd, P.M.; Al-Harbi, N.M.; Fritsch, D.; Heinrich, K.; Starannikova, L.; Tokarev, A.; Yampolskii, Y. Synthesis , Characterization , and Gas Permeation Properties of a Novel Group of Polymers with Intrinsic Microporosity : PIM-Polyimides. *Macromolecules* **2009**, *42*, 7881–7888.
23. Ghanem, B.S.; Mckeown, N.B.; Budd, P.M.; Selbie, J.D.; fritsch, D. High-Performance Membranes from Polyimides with Intrinsic Microporosity. *Adv. Mater.* **2008**, *20*, 2766–2771.
24. Zhang, Q.; Chen, G.; Zhang, S. Synthesis and Properties of Novel Soluble Polyimides having a Spirobisindane-Linked Dianhydride Unit. *Polymer*, **2007**, *48*, 2250–2256.
25. Rogan, Y.; Starannikova, L.; Ryzhikh, V.; Yampolskii, Y.; Bernardo, P.; Bazzarelli, F.; Jansen, J.C.; Mckeown, N.B. Synthesis and Gas Permeation Properties of Novel Spirobisindane-based Polyimides of Intrinsic Microporosity. *Polym. Chem*. **2013**, *4*, 3813–3820.
26. Liu, J.; Xiao, Y.; Liao, K.; Chung, T. Highly Permeable and Aging Resistant 3D Architecture from Polymers of Intrinsic Microporosity Incorporated with Beta-Cyclodextrin. *J. Memb. Sci.* **2017**, *523*, 92–102.
27. Swaidan, R.; Ma, X.; Litwiller, E.; Pinnau, I. High Pressure Pure- and Mixed-Gas Separation of CO_2/CH_4 by Thermally-Rearranged and Carbon Molecular Sieve Membranes Derived from a Polyimide of Intrinsic Microporosity. *J. Memb. Sci.* **2013**, *447*, 387–394.
28. Du, N.; Dal-Cin, M.M.; Robertson, G.P.; Guiver, M.D. Decarboxylation-Induced Cross-Linking of Polymers of Intrinsic Microporosity (PIMs) for Membrane Gas Separation. *Macromolecules* **2012**, *45*, 53078.
29. Swaidan, R.; Ghanem, B.S.; Litwiller, E.; Pinnau, I. Pure- and Mixed-Gas CO_2 /CH_4 Separation Properties of PIM-1. *J. Memb. Sci.* **2014**, *457*, 95–102.
30. Wu, X.M.; Zhang, Q.G.; Lin, P.J.; Qu, Y.; Zhu, A.M.; Liu, Q.L. Towards Enhanced CO_2 Selectivity of the PIM-1 Membrane by Blending with Polyethylene Glycol. *J. Memb. Sci.* **2015**, *493*, 147–155.
31. Ricci, E.; de Angelis, M.G. Modelling Mixed-Gas Sorption in Glassy Polymers for CO_2 Removal : A Sensitivity Analysis of the Dual Mode Sorption Model. *Membranes* **2019**, 9, 1–26.

32. Polak-Kkrasna, K.; Dawson, R.; Holyfield, L.T.; Bowen, C.R.; Burrows, A.D.; Mays, T.J. Mechanical Characterisation of Polymer of Intrinsic Microporosity PIM-1 for Hydrogen Storage Applications. *J. Mater. Sci.* **2017**, 52, 3862–3875